PERGAMON

International Journal of Heat and Mass Transfer 42 (1999) 2897–2903

International Journal of HEAT and MASS TRANSFER

Effects of vertical fins on local heat transfer performance in a horizontal fluid layer

Shigeaki Inada[a], Tsuyoshi Taguchi[a], Wen-Jei Yang[b,*]

[a] *Department of Mechanical System Engineering Gunma University, Kiryu City, Gunma 376, Japan*
[b] *Department of Mechanical Engineering and Applied Mechanics, University of Michigan, Ann Arbor, MI 48109, U.S.A.*

Received 29 September 1997; in final form 6 October 1998

Abstract

Enhancement of natural convection heat transfer in a horizontal fluid layer is an important problem pertinent to suppression of thermal stratification inside low-temperature liquid storage tanks. The experiments are carried out with an air layer between horizontal plates of aspect ratio 8.4, of which the bottom surface is isothermally heated, the upper surface is cooled at a constant room temperature and the vertical side wall are adiabatic. Some visualized results are reported of flow and temperature fields induced by natural convection in a horizontal fluid layer of finite extent; the former is measured with the laser light sheet methods and the latter with the holographic interferometry. The effects of partition intervals attached to the bottom surface and the Rayleigh number on local Nusselt numbers are discussed. It is disclosed that (1) increases in the Rayleigh number result in enhancement of the vortex convection and the heat transfer performance improves, (2) upward flows are created at the fin positions, and the heat transfer is enhanced to the greatest extent when downward flows occur between the fins, and (3) there is the optimum pitch of the partitions to enhance the heat transfer effects.

1. Introduction

The Rayleigh–Benard convection process that arises in horizontal fluid layers is pertinent to a wide variety of applications, including: the suppression of thermal stratification inside low-temperature liquid and liquefied gas storage tanks, temperature uniformity within a fluid during crystal formation, and fluid flows occurring during the cooling of electronic devices. Consequently, a large amount of research on this form of convection has been recorded. For example, Akiyama et al. [1] investigated the critical Rayleigh number at which Benard convection began to start. Mukutmoni and Yang [2] and Leith [3] studied the bifurcation to oscillatory convection. Busse and Clever [4] reported the growth of the oscillatory instability within the fluid layer with increasing the Rayleigh number. Globe and Dropkin [5] experimentally investigated heat transfer characteristics in the range of high Rayleigh numbers. As for flow pattern, Hasnaoui et al. [6] and Wang and Robillard [7] reported the numerical study of natural convection in a cavity with localized heating from below.

This report focuses primarily on natural convection fields roughly corresponding to the Rayleigh–Benard convection regions of horizontal fluid layers with the objective of gaining an understanding on how to enhance or how to reduce natural convection. Partitions, that is, fins were inserted within a fluid layer and a laser sheet method and holographic interferometry were used to visualize fluid flow near the partitions, as well as the temperature fields. In this study, the pitch of the partitions was varied and the effect on the local heat transfer characteristics was investigated experimentally.

This study fulfils the demand for precise temperature field visualization and quantification. Currently, to the best of the authors' knowledge, there has been no work performed in this area.

2. Experimental apparatus and procedure

Figure 1 shows an outline of the experimental apparatus. The height H (in the y direction) of the horizontal

* Corresponding author.

0017–9310/99/$ - see front matter
PII: S0017-9310(98)00357-3

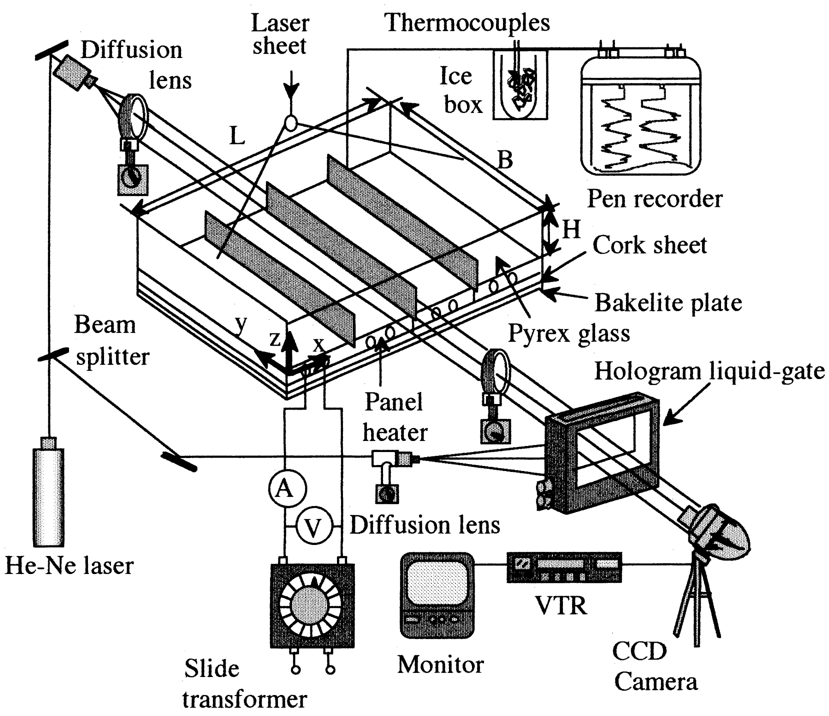

Fig. 1. Experimental apparatus.

fluid layer is 20 mm, the length (along the x-axis) is 168 mm, and the breadth B (along the z-axis) is 123 mm, forming a rectangular volume with an aspect ratio LH of 8.4.

The bottom surface of the fluid layer consists of a copper plate $168 \times 123 \times 2$ mm in size, heated from below by a Nichrome wire panel heater (150 W). The back of the panel heater is insulated with a cork sheet and a Bakelite plate, and shielded from the outside air with KAO-wool insulation. Pyrex glass sheets form the upper surface and long side surfaces (x–y plane) of the fluid layer, 2 mm in thickness. The short side surfaces (y–z plane) are constructed from Bakelite plates, with cork sheeting wedged under the lower edges in contact with the heated surface, to reduce heat loss through the Bakelite plates.

Copper–constantan thermocouples of diameter 0.05 mm are mounted directly on the heated surface at eight locations to measure the uniformity of the temperature of the bottom surface, T_h, and to confirm that the maximum temperature deviation is within 0.2 K. The glass forming the upper surface is maintained at constant room temperature by circulating the city water of a constant temperature. Copper-constantan thermocouples of 0.05 mm diameter are mounted directly on the inner surface of the glass and are used to verify the uniformity of the temperature, T_c. To investigate the heat transfer effect in relation to the partition arrangement, 1-mm thick copper plates and balsa plates are attached to the heated surface, parallel to the shorter sides and perpendicular to the bottom surface. The height of the partitions is 10 mm. The partitions are equally spaced, at intervals of 42 mm for three partitions, 28 mm for five partitions and 21 mm for seven partitions. The results are compared to the case where no partitions were used.

After setting up the optical system, the isotherms were visualized using holography. A holographic plate was exposed without the experimental fluid layer, and a hologram was created. Next, heating was started and after verifying that the temperature of each part had stabilized, a CCD camera was set behind the hologram and real-time images were recorded. In this experiment, the measurement field of the hologram was 80 mm, so the entire system was shifted horizontally, and photographs were taken at three separate locations. In addition, when the photographs were actually being taken, the glass window was shifted as little as possible, so as to be just outside the measurement field in order to avoid introducing interference fringes from glass distortion in the observation window.

Since the working fluid is air, smoke from an incense stick was introduced in order to visualize the Rayleigh–Benard convection, and reflected light from the laser sheet in the smoke was photographed. The flow field in the central cross-section of the fluid layer was visualized.

3. Evaluation of the measurement error of the local Nusselt number

The images of the interference fringes were fed into a computer to evaluate the local Nusselt numbers, Nu_H, using

$$Nu_H = \frac{H}{\delta}\frac{T_h - T_i}{T_h - T_c} \tag{1}$$

Here, the temperature T_i was a value measured using a 0.5 mm diameter chromel–alumel sheath-type thermocouple simultaneously with the recording of the interference fringe images and δ is the distance between the interference fringes and the heated surface. The distance δ indicates the variation in the rate of heat transfer, the shorter the distance, the better the heat transfer.

Factors contributing to measurement errors in equation (1) are the temperature measurement in the interference fringe and the distance measurement between the interference fringe nearest to the heated surface and the heated surface itself. A sheath-type thermocouple was used, and the following method was employed to evaluate the measurement error during the temperature measurement in the interference fringe. At least two interference fringes extending across the entire layer were created in the fluid layer (this was realized by setting $Ra = 20\,000$), and the temperature difference between the two interference fringes was measured using the sheath-type thermocouple. This difference in the temperature measurement was in good agreement with the value calculated from the relationship between the fluid layer width, the wavelength of the laser, and the refractive index temperature gradient. However, the diameter of the probe of the sheath-type thermocouple is 0.5 mm while the maximum width of the interference fringe was about 4 mm. (Measurements were made with the probe placed at the center of the widest portion). This means that the temperature measurements of the interference fringe include an error of a maximum of 6%. The evaluation of the measurement error inherent in the distance measurements showed that the interference fringes described above had the widest portions of dark banding at the center, and the width became sharper and narrower near the walls. The maximum width was about 4 mm at approximately the center of the fluid layer (at a distance of about 10 mm from the heated surface). A traveling microscope capable of taking measurements to the second decimal place was used to make the distance measurements. It is considered that the measurement includes a maximum error of 20%. This means that the measured values for the local Nusselt number incorporate a maximum measurement error of 26%.

4. Results and discussion

4.1. Local Nusselt number and flow patterns for Rayleigh number 6000

Figure 2 shows the isotherms over the entire length L of the horizontal fluid layer obtained using holographic interferometry at $T_h = 31.1°C$ and $T_c = 22.6°C$. The temperature T_i was measured using a 0.5-mm diameter chromel–alumel sheath-type thermocouple simultaneously with the recording of the interference fringe images.

Figure 2 shows (1) the case of without fin at $T_i = 26°C$, (2) for the case of 3-copper fins and (3) for the case of 7-copper fins.

Figure 3 shows the corresponding flow patterns. Below each pattern is a sketch as well as the photo of the actual measurements obtained by the laser sheet method. When there are fins, the isothermal fringes are forced upward toward the top of the fins. When there are no fins, it is possible to observe six vortices of approximately equal size matching the aspect ratio $(1:1.4, \text{height}:\text{width})$ known to be conducive to the development of Benard vortices. The without fin shows the same isothermal patterns and flow patterns as those in the case of 3-fins. For the case of 3-fins, the positions of the fins are nearly the same as positions of the rising flow of vortices, and it is observed that the isotherms are forced upward at each fin position and there is a strong upward flow. As a result, there is a downward flow between the fins. In other words, the cooled air at the upper portion of the fluid layer flows downward toward the heated surface, which promotes heat transfer. This could be determined from the observation that the isotherms between the fins lie in close to the heated surface. In the case of 7-fins, the upward-directed flow is intensified at each fin position, but the fin pitch does not match the aspect ratio of $1:1.4$ that leads to vortex formation. For this reason, there is interference in the upper portion of the fluid layer, and a strong downward flow like that seen in the case of 3-fins cannot be expected. However, compared to the case of without fin, there seems to be a greater fluid exchange between the upper and lower portions of the fluid layer between each partition.

The graphs of the local Nusselt numbers labeled (1), (2), and (3) in Fig. 4 correspond to (1), (2) and (3) in Figs 2 or 3, respectively. The images of the interference fringes were fed into a computer to evaluate the local Nusselt numbers, Nu_H, using equation (1).

The mean Nusselt number, Nu_m, over the entire length L of the fluid layer is indicated for $Ra = 6000$ in Fig. 4. In the case of without fin the value is 1.3, for 7-fins it is 1.7, and for 3-fins the value is 2.0. It is possible to consider that the heat transfer effect is enhanced by installation of fins for $Ra = 6000$. Large graduation marks shown on abscissa of (2) and (3) in Fig. 4 are placed to clearly show the positions of the fins. When there are fins, the local

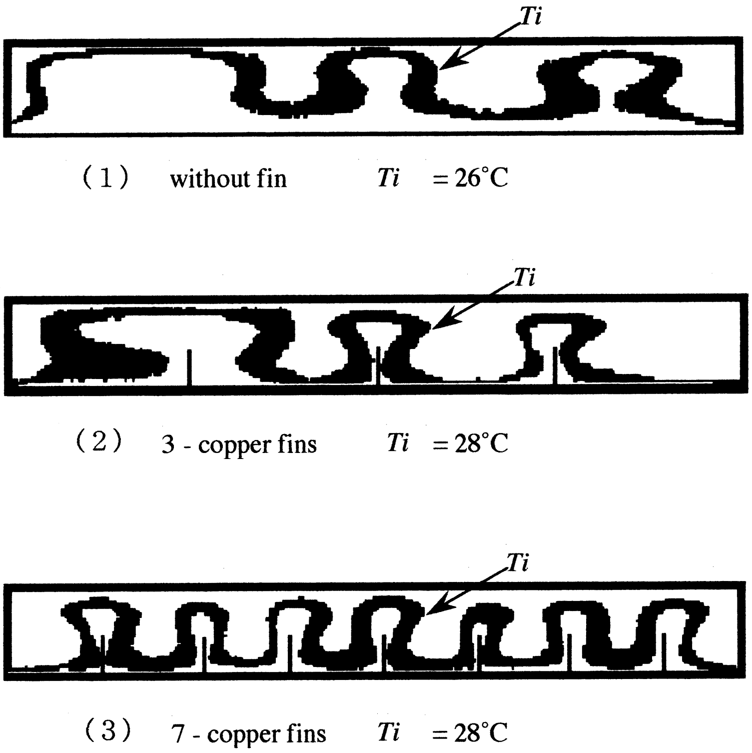

Fig. 2. Effects of fin pitch on isotherms for $Ra = 6000$.

Nusselt numbers show the minimum values of the same order at the fin positions and the maximum values at the middle of the fin spacing. Specially, in the case of 3-fins, the order of the maximum values of the local Nusselt number is the most high, so significant improvement of the heat transfer is recognized. Then the existence of a strong downward fluid flow between the fins can be considered. There is a slight difference between the maximum values in the left-hand side of a fin and in the right-hand side of the fin. This seems to be influenced by the instability of the Rayleigh–Benard convection.

4.2. Effects of Rayleigh number and fin pitch on average Nusselt number

Figure 5(a) and (b) shows the effects of the pitch of the fins on the isotherms in the central part ($2.5 < x/H < 7.0$) of the horizontal fluid layer obtained using holographic interferometry for the Rayleigh number 20 000.

Figure 5(a) shows the case of the conductive fins (copper) and (b) shows the case for the adiabatic fins (balsa plate, heat conductivity of 0.1 W/m K). (1) Figure 5(a) shows the case of without fin; (2) Fig. 5(a) and (b) shows the case of 3-fins; (3) Fig. 5(a) and (b) shows the case of 5-fins and (4) Fig. 5(a) and (b) shows the case of 7-fins. The isothermal patterns like that seen in Fig. 2 can be identified in both cases of the copper and balsa fins. However, in the case of without fin, (1) Fig. 5(a), eight vortices formed and active upward and downward flows were observed. The isotherms become thinner than the isotherms when $Ra = 6000$. Then, as the Rayleigh number was increased, the heat transfer performance improved. This is probably because the mixing within the fluid layer is further enhanced when there are eight vortices instead of six. For 3-fins and 7-fins, the flow patterns and the number of the vortices were the same as for $Ra = 6000$. However, the flow velocity, that is, vortex flow with ascending and descending streams in the fluid layer may be slightly faster, so the isotherms become thinner than when $Ra = 6000$. Accordingly, the heat transfer performance is even better than that when $Ra = 6000$. In the case of 5-fins and 7-fins for balsa plate, the isothermal lines are not forced upward toward the top of the fins at some fin positions. The reason can be considered that the upward flow collided with the downward flow at the fin positions resulting in counterflow and the isotherms at the top of the fins were suppressed by the downward flow.

In Figs 6(a) and (b) the average Nusselt number is plotted against the Rayleigh number with the number of fins as a parameter, the former is the case of the copper

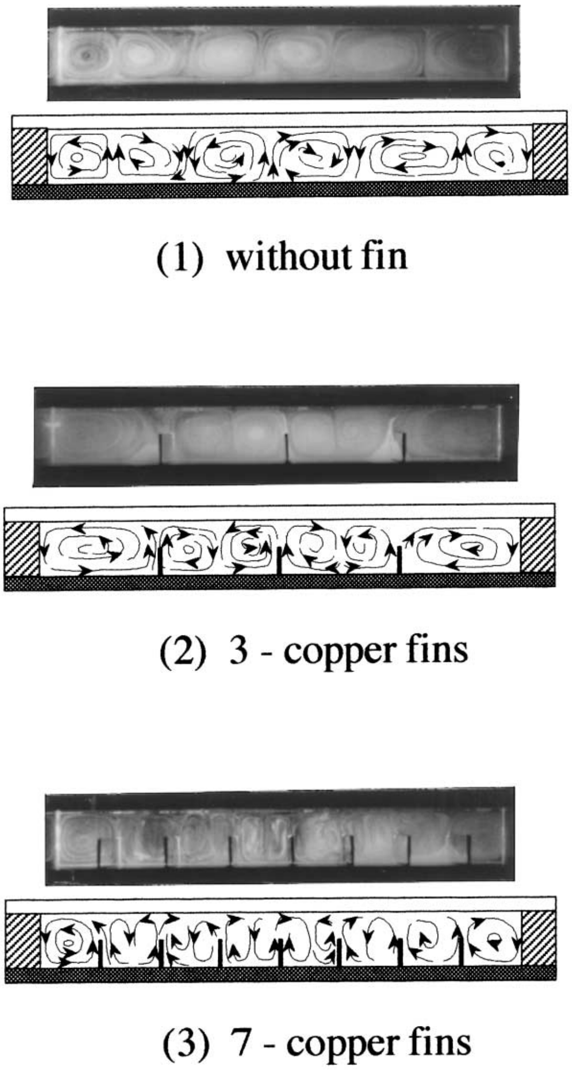

Fig. 3. Effects of fin pitch on flow patterns for $Ra = 6000$.

fins and the latter is for the balsa fins. As the Rayleigh number is increased, the heat transfer performance improves. We can confirm that the measurements for both the copper and balsa fins show the greatest improvement in the heat transfer performance when 3-fins are used. The reason for this enhancement is referred to the mechanism mentioned in the previous section; that is, the reason is that upward flows are created at the fin positions when downward flows occur between the fins. In the case of copper fin, the order of high Nusselt number is that of 3-fins, without fin or 5-fins and 7-fins. On the other hand, in the case of balsa fin, 3-fins and 5-fins show higher values than for without fin. However, as is evident from Fig. 6(b), for the case of 7-fins, the effect of heat transfer augmentation is reduced compared to that of without fin. The reason for this reduction in heat transfer can be

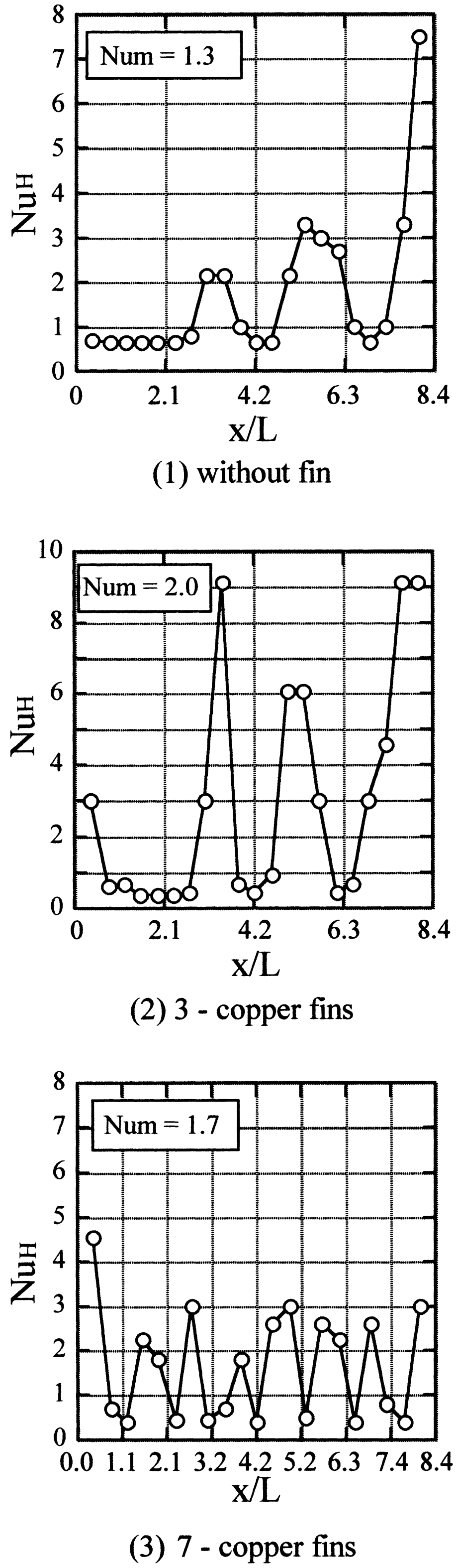

Fig. 4. Effects of fin pitch on the local Nusselt number for $Ra = 6000$.

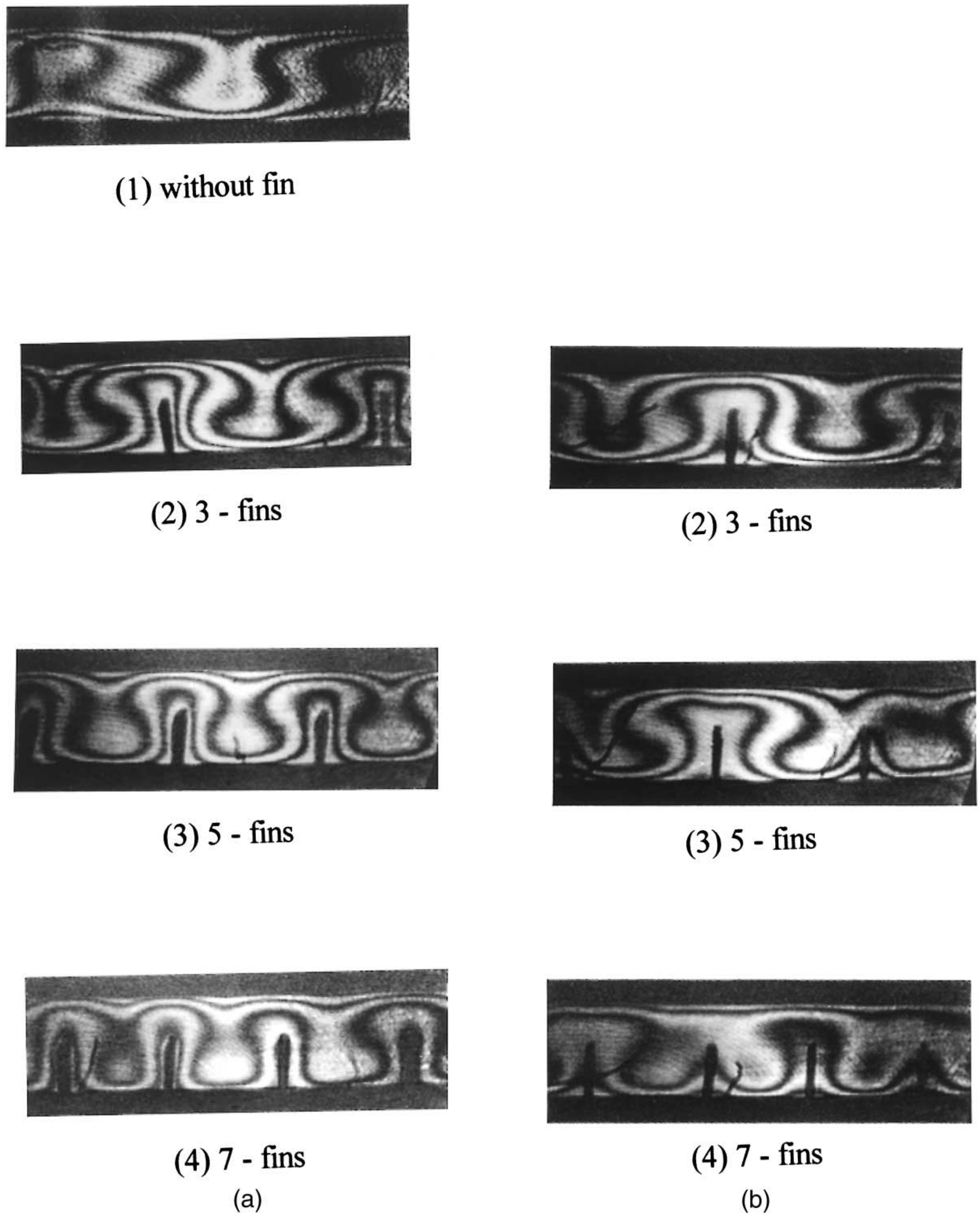

Fig. 5. (a) Effects of fin pitch on isotherms for copper fins and $Ra = 20\,000$; (b) effects of fin pitch on isotherms for balsa fins and $Ra = 20\,000$.

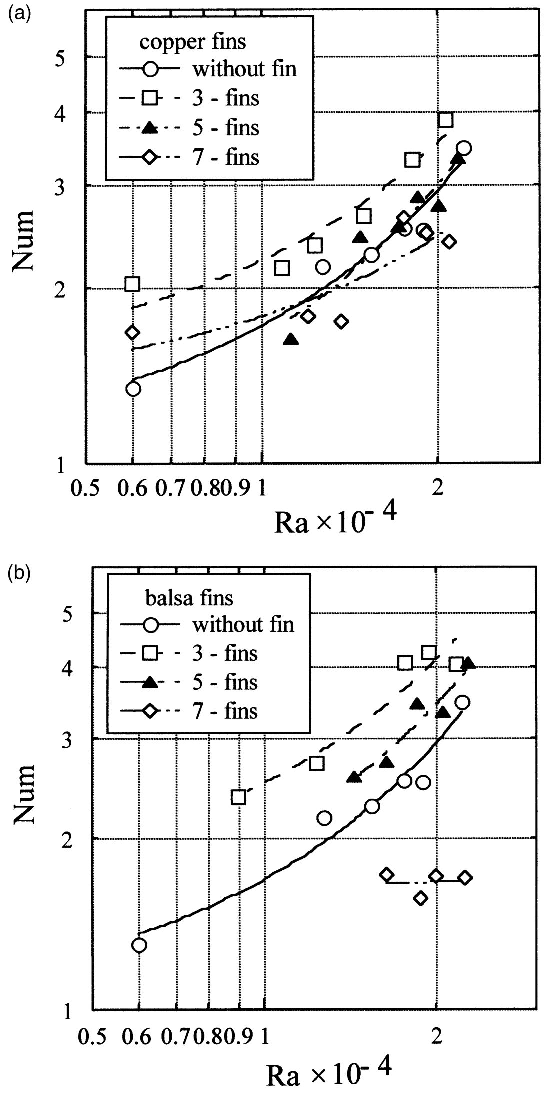

Fig. 6. (a) Effects of Rayleigh number and fin pitch on the average Nusselt number in the case of copper fins; (b) effects of Rayleigh number and fin pitch on the average Nusselt number in the case of balsa fins.

considered that the fluid flow between the fins is sluggish along the heated surface because of restricted space, so that the downward flow is weakened and heat transfer is worse than for without fin. Bearing in mind the accuracy of the measurement values, it is possible to consider that the fin material does not significantly affect the characteristics indicated by the value of the average Nusselt number vs the Rayleigh number.

5. Conclusions

(1) Increases in the Rayleigh number result in enhancement of the vortex convection and the heat transfer performance improves.
(2) Upward flows are created at the fin positions, and the heat transfer is enhanced to the greater extent when downward flows occur between the fins.
(3) By placing fins at the aspect ratio positions to form stable Rayleigh–Benard convection, the vortex convection effect is enhanced, so that it is possible to expect an improvement in the heat transfer compared to the case of without fin.

References

[1] M. Akiyama, G.J. Hwang, K.C. Cheng. Experiments on the onset of longitudinal vortices in laminar forced convection between horizontal plates. ASME Journal of Heat Transfer 93 (1971) 335–341.
[2] D. Mukutmoni, K.T. Yang. Rayleigh–Benard convection in a small aspect ratio enclosure; part I bifurcation to oscillatory convection. ASME Journal of Heat Transfer 115 (1993) 360–366.
[3] J.R. Leith. Flow Structure Transition Mechanisms in Thermal Convection of Air in Rectangular Containers. Physica D 37, North-Holland, Amsterdam, 1989. pp. 334–340.
[4] F.H. Busse, R.M. Clever. Instabilities of convection rolls in a fluid of moderate Prandtl number. J. Fluid Mechanics 91 (1979) 319–335.
[5] S. Globe, D. Dropkin. Natural convection heat transfer in liquids confined by two horizontal plates and heated from below. ASME Journal of Heat Transfer 81 (1959) 24–28.
[6] M. Hasnaoui, E. Bilgen, P. Vasseur. Multiplicity of solutions and heat transfer by natural convection in a rectangular cavity partially heated from below. ASME/JSME Thermal Engineering Proceedings 1 (1991) 69–75.
[7] X. Wang, L. Robillard. Mixed convection in a horizontal layer: the moving window approach. ASME/JSME Thermal Engineering Proceedings 1 (1991) 9–16.